

# Electric quadrupole moment of the $4d\ ^2D_{5/2}$ state in $^{88}\text{Sr}^+$ and its role in an optical frequency standard

Chiranjib Sur, K. V. P. Latha, Rajat K. Chaudhuri, B. P. Das

*Non-Accelerator Particle Physics Group, Indian Institute of Astrophysics, Bangalore - 560 034, India*

D. Mukherjee

*Department of Physical Chemistry, Indian Association for the Cultivation of Science, Kolkata - 700 032, India*

The electric quadrupole moment for the  $4d\ ^2D_{5/2}$  state of  $^{88}\text{Sr}^+$ , one of the most important candidates for an optical clock, has been calculated using the relativistic coupled-cluster theory. The result of the calculation is presented and the important many-body contributions are highlighted. The calculated electric quadrupole moment is  $(2.94 \pm 0.07)ea_0^2$ , where  $a_0$  is the Bohr radius and  $e$  the electronic charge while the measured value is  $(2.6 \pm 0.3)ea_0^2$ . This is so far the most accurate determination of the electric quadrupole moment for the above mentioned state.

PACS numbers: 31.15.Ar, 31.15.Dv, 32.30.Jc

The frequencies at which atoms emit or absorb electromagnetic radiation during a transition can be used for defining the basic unit of time [1, 2, 3]. The transitions that are extremely stable, accurately measurable and reproducible can serve as excellent frequency standards [1, 2]. The current frequency standard is based on the ground state hyperfine transition in  $^{133}\text{Cs}$  which is in the microwave regime and has an uncertainty of one part in  $10^{15}$  [4]. However, demands from several areas of science and technology have lead to a worldwide search [5] for even more accurate clocks in the optical regime. The uncertainty of these clocks is expected to be about 1 part in  $10^{17}$  or  $10^{18}$  [5]. Some of the prominent candidates that belong to this category are  $^{199}\text{Hg}^+$  [6],  $^{88}\text{Sr}^+$  [7, 8],  $^{171}\text{Yb}^+$  [9] etc. Indeed detailed studies on these ions will have to be carried out in order to determine their suitability for optical frequency standards. In a recent article [10] Gill and Margolis have discussed the merits of choosing  $^{88}\text{Sr}^+$  as a candidate for an optical clock. Till recently, the most accurate measurement of an optical frequency was for the clock transition in  $^{88}\text{Sr}^+$  which has an uncertainty of 3.4 parts in  $10^{15}$  [11]. However, recently, Oskay et al. [12] have measured the optical frequency of  $^{199}\text{Hg}^+$  to an accuracy of 1.5 parts in  $10^{15}$  and further improvements are expected [13].

When an atom interacts with an external field, the standard frequency may be shifted from the resonant frequency [14]. The quality of the frequency standard depends upon the accurate and precise measurement of this shift. To minimize or maintain any shift of the clock frequency, the interaction of the atom with its surroundings must be controlled. Hence, it is important to have a good knowledge of these shifts so as to minimize them while setting up the frequency standard. Some of these shifts are the linear Zeeman shift, quadratic Zeeman shift, second-order Stark shift and electric quadrupole shift due to the interaction of atomic electric quadrupole moment with the gradient of electric field [14]. The largest source of uncertainty in frequency shift arises from the electric quadrupole shift of the clock transition. The electric

quadrupole moments of  $^{88}\text{Sr}^+$ ,  $^{199}\text{Hg}^+$  and  $^{171}\text{Yb}^+$  have been measured in order to determine this shift. However, accurate measurements of these shifts are very difficult. The calculation of these shifts although very challenging could in some cases be more accurate than the measurements. Such calculations have received relatively less attention so far. The most rigorous calculation to date has been performed by Oskay et al [12] for  $^{199}\text{Hg}^+$  using the relativistic configuration interaction (RCI) method with a multi-configuration Dirac-Fock - extended optimized level (MCDF-EOL) orbital basis. We focus on the clock transition  $5s\ ^2S_{1/2} - 4d\ ^2D_{5/2}$  in  $^{88}\text{Sr}^+$  in the present paper. Figure 1 shows the clock transition in  $^{88}\text{Sr}^+$ . The electric quadrupole moment in the state  $4d\ ^2D_{5/2}$  was measured experimentally by Barwood *et al.* at NPL [15]. Since the ground state  $5s\ ^2S_{1/2}$  does not possess any electric quadrupole moment, the contribution to the quadrupole shift for the clock frequency comes only from the  $4d\ ^2D_{5/2}$  state. In this letter, we present our rela-

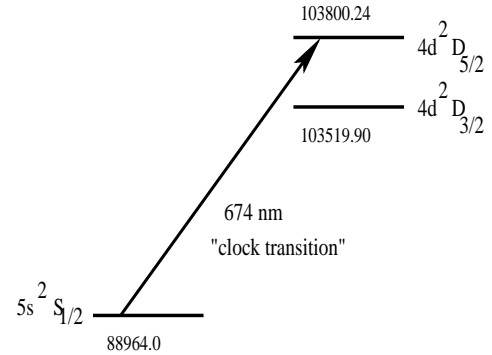


FIG. 1: Diagram indicating the clock transition in  $^{88}\text{Sr}^+$ . Energy levels are given in  $\text{cm}^{-1}$ .

tivistic coupled-cluster (RCC) calculation of the electric quadrupole moment of  $^{88}\text{Sr}^+$  in the  $4d\ ^2D_{5/2}$  state. RCC is equivalent to all-order relativistic many-body perturbation theory (RMBPT).

The details of this theory have been discussed in several

articles [16, 17]. Here we shall only give a brief outline. Treating the closed shell Dirac-Fock (DF) state  $|\Phi\rangle$  as the reference state, the exact wave function in RCC theory can be expressed as,

$$|\Psi\rangle = \exp(T) |\Phi\rangle, \quad (1)$$

where  $T$  is the core electron excitation operator. In the coupled cluster singles and doubles (CCSD) approximation,  $T$  can be expressed as the sum of one- and two-body excitation operators, *i.e.*  $T = T_1 + T_2$ , and can be written in the second quantized form as

$$T = T_1 + T_2 = \sum_{ap} a_p^\dagger a_a t_a^p + \frac{1}{2} \sum_{abpq} a_p^\dagger a_q^\dagger a_b a_a t_{ab}^{pq}. \quad (2)$$

where  $t_a^p$  and  $t_{ab}^{pq}$  are the amplitudes of the singles and double excitation operators respectively. The normal ordered Hamiltonian can be written as,

$$H_N \equiv H - \langle \Phi | H | \Phi \rangle = H - E_{DF}, \quad (3)$$

where  $H$  is the Dirac-Coulomb Hamiltonian given by

$$H_{DC} = \sum_i^N [c\alpha_i \cdot \mathbf{p}_i + \beta_i c^2 + V(r_i)] + \sum_{i<j} \frac{1}{r_{ij}} \quad (4)$$

For a single valence system we define the reference state as,

$$|\Phi_v^{N+1}\rangle \equiv a_v^\dagger |\Phi\rangle \quad (5)$$

with the particle creation operator  $a_v^\dagger$ . The wave function corresponding to this state can be written as,

$$|\Psi_v^{N+1}\rangle = \exp(T) \{(1 + S_v)\} |\Phi_v^{N+1}\rangle. \quad (6)$$

where,

$$S_v = S_{1v} + S_{2v} = \sum_{v \neq p} a_p^\dagger a_v s_v^p + \sum_{bpq} a_p^\dagger a_q^\dagger a_b a_v s_{vb}^{pq}, \quad (7)$$

where  $S$  corresponds to the excitation operator in the valence sector and  $v$  stands for valence orbital and  $s_v^p$  and  $s_{vb}^{pq}$  are the amplitudes of single and doubles excitations respectively. Details concerning the evaluation of the closed and open shell amplitudes have been discussed earlier [18]. Triple excitations are included in our open shell RCC amplitude calculations in an approximate way (CCSD(T)) [19].

The expectation value of any operator  $O$  with respect to the state  $|\Psi^{N+1}\rangle$  is given by,

$$\begin{aligned} \langle O \rangle &= \frac{\langle \Psi^{N+1} | O | \Psi^{N+1} \rangle}{\langle \Psi^{N+1} | \Psi^{N+1} \rangle} \\ &= \frac{\langle \Phi^{N+1} | \{1 + S^\dagger\} \bar{O} \{1 + S\} | \Phi^{N+1} \rangle}{\langle \Phi^{N+1} | \{1 + S^\dagger\} \exp(T^\dagger) \exp(T) \{1 + S\} | \Phi^{N+1} \rangle} \end{aligned} \quad (8)$$

where  $\bar{O} = \exp(T^\dagger) O \exp(T)$ .

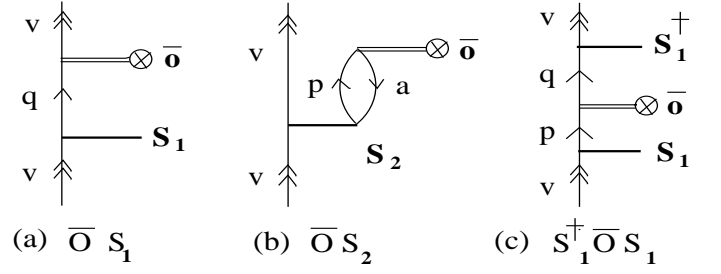


FIG. 2: The diagrams (a) and (c) are subsets of dressed pair correlation (DPC) diagrams. Diagram (b) is one of the direct dressed core-polarization (DCP) diagram.

The first few terms in the above expectation value can be identified as  $\bar{O}$ ,  $\bar{O}S_1$ ,  $\bar{O}S_2$ ,  $S_1^\dagger \bar{O}S_1$  etc; are referred to as dressed Dirac-Fock (DDF), dressed pair correlation (DPC) (Fig.2(a)) and dressed core polarization (DCP) (Fig.2(b)) respectively. We use the term ‘dressed’ because the operator  $O$  includes the effects of the core excitation operator  $T$ . Among the above, we can identify few other terms which play crucial role in determining the correlation effects. One of those terms is  $S_1^\dagger \bar{O}S_1 + c.c$  ((Fig.2(c)) which is called as dressed higher order pair correlation (DHOPC) since it directly involves the correlation between a pair of electrons. In table II individual contributions from these diagrams are listed.

The orbitals used in the present work are expanded in terms of a finite basis set comprising of Gaussian type orbitals (GTO) [20]

$$F_{i,k}(r) = r^k \exp(-\alpha_i r^2), \quad (9)$$

with  $k = 0, 1, 2 \dots$  for  $s, p, d, \dots$  type functions, respectively. The exponents are determined by the even tempering condition [21]

$$\alpha_i = \alpha_0 \beta^{i-1}. \quad (10)$$

The starting point of the computation is the generation of the Dirac-Fock (DF) orbitals [20] which are defined on a radial grid of the form

$$r_i = r_0 [\exp(i-1)h - 1] \quad (11)$$

with the freedom of choosing the parameters  $r_0$  and  $h$ . All DF orbitals are generated using a two parameter Fermi nuclear distribution

$$\rho = \frac{\rho_0}{1 + \exp((r - c)/a)}, \quad (12)$$

where the parameter  $c$  is the half charge radius and  $a$  is related to skin thickness, defined as the interval of the nuclear thickness in which the nuclear charge density falls from near one to near zero. The interaction of the atomic quadrupole moment with the external electric-field gradient is analogous to the interaction of a nuclear quadrupole moment with the electric fields generated by the atomic electrons inside the nucleus. In the presence

of the electric field, this gives rise to an energy shift by coupling with the gradient of the electric field. Thus the treatment of electric quadrupole moment is analogous to the nuclear counterpart. The quadrupole moment  $\Theta$  of an atomic state  $|\Psi(\gamma, J, M)\rangle$  is defined as the diagonal matrix element of the quadrupole operator with the maximum value  $M_J$ , given by,

$$\Theta = \langle \Psi(\gamma J J) | \Theta_{zz} | \Psi(\gamma J J) \rangle. \quad (13)$$

Here  $\gamma$  is an additional quantum number which distinguishes the initial and final states. The electric quadrupole operator in terms of the electronic coordinates is given by,

$$\Theta_{zz} = -\frac{e}{2} \sum_j (3z_j^2 - r_j^2),$$

where the sum is over all the electrons and  $z$  is the coordinate of the  $j$ th electron. To calculate the quantity we express the quadrupole operator in its single particle form as

$$\Theta_m^{(2)} = \sum_m q_m^{(2)} \quad (14)$$

and the single particle reduced matrix element is expressed as [22]

$$\langle j_f \| q_m^{(2)} \| j_i \rangle = \langle j_f \| C_m^{(2)} \| j_i \rangle \frac{15}{k^2} \int dr \left\{ j_2(kr) (P_{\kappa_f} P_{\kappa_i} + Q_{\kappa_f} Q_{\kappa_i}) + j_3(kr) \frac{(j_j - j_i - 1)}{3} (P_{\kappa_f} Q_{\kappa_i} + Q_{\kappa_f} P_{\kappa_i}) \right\}. \quad (15)$$

In Eq.(15), the subscripts  $f$  and  $i$  correspond to the final and initial states respectively and  $j_m(kr)$  is the Bessel function of order  $m$ ;  $P$  and  $Q$  are the radial part of the large and small components of the single particle Dirac-Fock wavefunctions respectively.  $j_i$  is the total angular momentum and  $\kappa_i$  is the relativistic angular momentum quantum number for the  $i$ th electron. The angular factor is given by

$$\begin{aligned} \langle j_f \| C_m^{(k)} \| j_i \rangle = & (-1)^{(j_f+1/2)} \sqrt{(2j_f+1)} \sqrt{(2j_i+1)} \\ & \times \begin{pmatrix} j_f & 2 & j_i \\ -1/2 & 0 & 1/2 \end{pmatrix} \pi(l, k, l') \end{aligned} \quad (16)$$

where

$$\pi(l, k, l') = \begin{cases} 1 & \text{if } l + k + l' \text{ even} \\ 0 & \text{otherwise} \end{cases}$$

$l$  and  $k$  being the orbital angular momentum and the rank respectively.

Finally using the Wigner Eckart theorem we define the electric quadrupole moment in terms of the reduced matrix elements as

$$\langle j_f | \Theta_m^{(2)} | j_i \rangle = (-1)^{j_f - m_f} \begin{pmatrix} j_f & 2 & j_i \\ -m_f & 0 & m_f \end{pmatrix} \langle j_f \| \Theta^{(2)} \| j_i \rangle \quad (17)$$

In table I we have presented the details of the basis functions used in this calculation and in table II contributions from different many body terms. The value of  $\Theta$  in the  $4d^2 D_{5/2}$  state measured experimentally is  $(2.6 \pm 0.3)ea_0^2$  [15], where  $e$  is the electronic charge and  $a_0$  is the Bohr radius. Our calculated value for the  $4d^2 D_{5/2}$  stretched state is  $(2.94 \pm 0.07)ea_0^2$ . We have estimated the error incurred in our present work, by taking

the difference between our RCC calculations with singles, doubles as well as the most important triple excitations (CCSD(T)) and only single and double excitations (CCSD). A non-relativistic Hartree-Fock (HF) determination resulted in  $\Theta = 3.03ea_0^2$  [15]. A subsequent calculation based on RCI with MCDF-EOL orbital basis yielded  $\Theta = 3.02ea_0^2$  [12]. In that calculation, correlation effects arising from a subset of the terms  $S_1$ ,  $T_1$  for single excitations and  $S_2$  and  $T_2$  for double excitations were considered, where  $S_1$  and  $S_2$  are the cluster operators representing single excitations from the valence  $5s$  orbital to a virtual orbital and double excitations from the valence  $5s$  and the core  $\{4s, 4p, 3d\}$  orbitals, with atmost one excitation from the core, respectively. In our calculation, in addition to these effects, the effects arising from the non-linear terms like  $T_2^2$ ,  $T_1 T_2$ , etc. have been included. In the framework of CCSD theory, the single and double excitations have been treated to all orders in electron correlation including excitations from the entire core. This amounts to a more rigorous treatment of electron correlation in comparison to the previous calculation performed using the RCI method..

It is clear from the table II that the DDF contribution is the largest. The leading correlation contribution comes from the DPC effects and the DCP effects are an order of magnitude smaller. This can be understood from the DPC diagram (Fig.2(a)) which has a valence electron in the  $4d_{5/2}$  state. Hence the dominant contribution to the electric quadrupole moment arises from the overlap between virtual  $d_{5/2}$  orbitals and the valence, owing to the fact that  $S_1$  is an operator of rank 0 and the electric quadrupole matrix elements for the valence  $4d_{5/2}$  and the diffuse virtual  $d_{5/2}$  orbitals are substantial. On the other hand, in the DCP diagram (Fig.2(b)), the matrix

TABLE I: No. of basis functions used to generate the even tempered Dirac-Fock orbitals and the corresponding value of  $\alpha_0$  and  $\beta$  used.

	$s_{1/2}$	$p_{1/2}$	$p_{3/2}$	$d_{3/2}$	$d_{5/2}$	$f_{5/2}$	$f_{7/2}$	$g_{7/2}$	$g_{9/2}$
Number of basis	38	35	35	30	30	25	25	20	20
$\alpha_0(\times 10^{-5})$	525	525	525	425	425	427	427	425	425
$\beta$	2.33	2.33	2.33	2.13	2.13	2.13	2.13	1.98	1.98
Active holes	10	10	10	11	11	8	8	6	6
Active particles	4	3	3	1	1	0	0	0	0

TABLE II: Contributions of the electric quadrupole moment in atomic units from different many-body effects in the CCSD(T) calculation. The terms like DDF, DCP, DPC, DHOPC are explained in the text. The remaining terms in Eq.8 are referred to as ‘others’.

DDF	DPC	DCP	DHOPC	Others	Total
3.4963	-0.4306	-0.0642	0.0353	-0.0271	2.94

element of the same operator could also involve the less diffuse  $s$  or  $p$  orbitals. Hence, for a property like the electric quadrupole moment, whose magnitude depends

on the square of the radial distance from the nucleus, this trend seems reasonable, whereas for properties like hyperfine interaction which is sensitive to the near nuclear region, the trend is just the opposite for the  $d$  states [23]. As expected, the contribution of the DHOPC effect i.e.,  $S_1^\dagger \bar{O} S_1$  (Fig.2(c)) is relatively important as it involves an electric quadrupole matrix element between the valence  $4d_{5/2}$  and a virtual  $d_{5/2}$  orbital. Unlike many other properties particularly the hyperfine interactions, an all-order determination of this diagram is essential for obtaining an accurate value of the electric quadrupole moment. One of the strengths of RCC theory is that it can evaluate such diagrams to all orders in the residual Coulomb interaction.

In conclusion, we have performed an *ab initio* calculation of the electric quadrupole moment for the  $4d^2 D_{5/2}$  state of  $^{88}\text{Sr}^+$  to an accuracy of less than 2.5 % using the RCC theory. Evaluation of correlation effects to all orders as well as the inclusion of the dominant triple excitations in our calculation was crucial in achieving this accuracy. This is currently the most accurate determination of electric quadrupole moment for this state in  $\text{Sr}^+$ . Our result will lead to a better quantitative understanding of the electric quadrupole shift of the resonance frequency of the clock transition in  $^{88}\text{Sr}^+$ .

This work was supported by the BRNS for project no. 2002/37/12/BRNS. The computations were carried out on our group’s Xeon PC cluster. We are grateful to Dr. Wayne Itano and Dr. Geoffrey Barwood, for helpful discussions.

- 
- |  |   |
|--|---|
| <p>[1] J.C. Bergquist, S. R. Jefferts, and D. J. Wineland, <i>Physics Today</i>, <b>54</b>, No.3, 37, (2001).</p> <p>[2] W.M. Itano, <i>Proc. IEEE</i>, <b>79</b>, 936-942 (1991).</p> <p>[3] W.M. Itano and N.F. Ramsey, <i>Sci. Am.</i>, <b>269</b>, 56-65 (1993).</p> <p>[4] <a href="http://tf.nist.gov/cesium/atomichistory.htm">http://tf.nist.gov/cesium/atomichistory.htm</a></p> <p>[5] L. Hollberg <i>et al.</i>, <i>J.Phys.B, At.Mol.Opt.Phys.</i>, <b>38</b>, S469-S495 (2005).</p> <p>[6] R. Rafac <i>et al.</i>, <i>Phys. Rev. Lett.</i> <b>85</b>, 2462 (2000).</p> <p>[7] J. E. Bernard <i>et al.</i>, <i>Phys. Rev. Lett.</i> <b>82</b>, 3228 (1999).</p> <p>[8] H. S. Margolis <i>et al.</i>, <i>Phys. Rev. A</i> <b>67</b>, 032501 (2003).</p> <p>[9] J. Stenger <i>et al.</i>, <i>Opt. Lett.</i> <b>26</b>, 1589 (2001).</p> <p>[10] P. Gill and H. Margolis, <i>Phys. World</i>, <b>18</b>, no. 5, 35 (2005).</p> <p>[11] H. S. Margolis <i>et al.</i>, <i>Science</i>, <b>306</b>, 1355 (2004).</p> <p>[12] W. H. Oskay, W. M. Itano and J. C. Bergquist, <i>Phys. Rev. Lett.</i> <b>94</b>, 163001 (2005).</p> <p>[13] W. M. Itano, NIST, <i>Private Communications</i>.</p> <p>[14] W. M. Itano, <i>J. Res. Natl. Inst. Stand. Technol.</i> <b>105</b>, 829 (2000).</p> <p>[15] G. P. Barwood <i>et al.</i>, <i>Phys. Rev. Lett.</i> <b>93</b>, 133001 (2004).</p> | <p>[16] R. F. Bishop, <i>Lecture Notes in Physics, Microscopic Quantum Many-Body Theories and their Applications</i>, p.1, Eds. J. Navarro and A. Polls, Springer-Verlag-Berlin, Heidelberg and New York (1998).</p> <p>[17] R. J. Bartlett, <i>Modern Electronic Structure Theory</i>, vol-II, p.1047, Ed. D. R. Yarkony, World Scientific, Singapore (1995).</p> <p>[18] G. Gopakumar, H. Merlitz, R.K. Chaudhuri, B.P. Das, U.S. Mahapatra, D. Mukherjee, <i>Phys. Rev.A.</i> <b>66</b>, 032505 (2002).</p> <p>[19] C.Sur, B.K. Sahoo, R.K. Chaudhuri, B.P. Das, and D. Mukherjee, <i>Eur.Phys.J.D</i> <b>32</b>, 25-31 (2005).</p> <p>[20] R. K. Chaudhuri, P. K. Panda and B. P. Das, <i>Phys. Rev. A</i>, <b>59</b>, 1187 (1999).</p> <p>[21] R. C. Raffanetti and K. Ruedenberg, <i>J. Chem. Phys.</i> <b>59</b>, 5978 (1973).</p> <p>[22] I. P. Grant, <i>J. Phys. B</i>, <b>7</b>, 1458 (1974).</p> <p>[23] C. Sur, B. K. Sahoo, R. K. Chaudhuri, B. P. Das and D. Mukherjee, <i>Euro. Phys. J. D</i>, <b>32</b>, 25 (2005).</p> |
|--|---|